Nanoscale Research Letters

NANO EXPRESS Open Access

Tailored Solid Polymer Electrolytes by Montmorillonite with High Ionic Conductivity for Lithium-Ion Batteries

Yingjian Zhao[1,2] and Yong Wang[1*]

Abstract

Polyethylene oxide (PEO)-based solid polymer electrolytes (SPEs) have important significance for the development of next-generation rechargeable lithium-ion batteries. However, strong coordination between lithium ions and PEO chains results the ion conductivity usually lower than the expectation. In this study, sub-micron montmorillonite is incorporated into the PEO frames as Lewis base center which enables the lithium ions to escape the restraint of PEO chains. After involving montmorillonite (MMT) into the SPEs, the ionic conductivity of SPEs is 4.7 mS cm^{-1} at 70 °C which shows a comparable value with that of liquid electrolyte. As coupling with $LiFePO_4$ material, the battery delivers a high discharge capacity of 150.3 mAh g^{-1} and an excellent rate performance with a capacity of 111.8 mAh g^{-1} at 0.16 C and maintains 58.2 mAh g^{-1} at 0.8 C. This study suggests that the customized incorporation of Lewis base materials could offer a promising solution for achieving high-performance PEO-based solid-state electrolyte.

Keywords: Solid polymer electrolyte, Lithium-ion battery, Electrochemical window, Montmorillonite, Lewis acid-base theory

Introduction

The requirements of energy storage devices for portable electronic [1], communication equipment [2], and hybrid electric vehicles are emerging [2–4]. Typically, the storage devices are proposed using lithium-ion batteries (LIBs), which have high specific energy, light weight, and easy to carry and quick to set up, as power sources to meet those fields [5–11]. However, for the commercial lithium-ion batteries, the liquid electrolyte systems suffer huge threats due to the flammability and the effects of a poison [5, 12, 13]. For instance, the boiling point of ethyl acetate, dimethyl carbonate, diethyl carbonate, and ethylene carbonate is only 77 °C, 90 °C, 127 °C, and 243 °C, respectively [5]. More importantly, the component material of commercial separators is polyethylene (PE) or polypropylene (PP), which will deform as the temperature up to 60 °C [14]. Therefore, once the operating temperature (> 60 °C) exceeds the critical temperature, the structure of separators will shrivel, resulting in inner short due to the lost function for physical dividing the cathode and anode [14, 15]. As compared, the solid electrolytes are worth expectation, they have the most competitive strategies to battle abovementioned issues because of thermal stability, chemical durability, and electrochemistry compatibility [16–19].

The inorganic solid electrolytes, such as sulfides (e.g., $Li_{10}GeP_2S_{12}$ [20], $Li_{9.54}Si_{1.74}P_{1.44}S_{11.7}Cl_{0.3}$ (25 mS cm^{-1}) [21], $Li_{11}Si_2PS_{12}$ [22]), oxides (e.g., $Li_{7+2x-y}(La_{3-x}Rb_x)(Zr_{2-y}Ta_y)O_{12}$ ($0 \le x \le 0.375$, $0 \le y \le 1$) [23], and $Li_7La_3Zr_2O_{12}$ [18]), show an exceptionally high conductivity. Some researchers reported that the lithium ion conductivity can reach up to 25 mS cm^{-1}, which is far higher than the conductivity of liquid electrolyte (~ 10^{-3} S cm^{-1}) [21]. However, for inorganic solid electrolytes, they show the poor mechanical properties with low Young's modulus and large number of grain boundaries within the inner of solid electrolyte [24], resulting in the failure for scale production [1].

Inorganic solid electrolyte combining with ion conductive polymer polyethylene oxide (PEO) has attracted

* Correspondence: ywang@uestc.edu.cn
[1]State Key Laboratory of Electronic Thin Films and Integrated Devices, University of Electronic Science and Technology of China, Chengdu 610054, China
Full list of author information is available at the end of the article

widespread concern for solid polymer electrolytes (SPEs) to overcome abovementioned issues due to the unique features that PEO has excellent mechanical stability, reliable film forming capability, especially, the good compatibility with the lithium metal anode [17, 25, 26]. However, due to the Lewis base performance of PEO, lithium ions tend to imprison on the PEO chains, resulting in low lithium ion conductivity [17, 27–29].

In this work, we introduce a small quantity of submicro montmorillonite as a Lewis base center into the SPEs where the montmorillonite can establish the coordinate with lithium ions because the montmorillonite serves as a competitor to compete the lithium ions [30]. As a result, the proposed SPEs deliver high ionic conductivity (4.7 mS cm^{-1}) at 70 °C and the prepared all solid lithium-ion battery coupling $LiFePO_4$ as cathode contributes discharge capacity of 150.3 mAh g^{-1} with the $LiFePO_4$ loading of 2 mg cm^{-2}, far exceeding the PEO-based solid electrolyte (119.1 mAh g^{-1}) at a current density of 0.08 C (1 C = 0.170 mAh g^{-1}).

Experimental Methods

Materials and Chemicals

For solid polymer electrolyte preparation, 500 mg PEO (Aladdin) and 250 mg lithium bis(trifluoromethanesulfonyl)imide (LITSFI, Aladdin) are dissolved into 10 mL acetonitrile (Aladdin), and then, 150 mg $Li_{6.4}La_3Zr_{1.4}Ta_{0.6}O_{12}$ (LLZTO, Tai'an Faraday Energy Technology Co., Ltd) is added into the PEO solution with fast stirring at 70 °C to ensure uniform distribution. Finally, the slurry is casted on the surface of the Teflon film and dried at 80 °C under Ar atmosphere. For comparison, the MMT-based solid electrolyte is prepared using same method except the montmorillonite (Aladdin) is additional added with the mass loading of 100 mg.

Characterization

Thermogravimetric (TG, Netzsch STA 449F3) analysis is performed for thermal stability with a heating rate of 10 °C min^{-1} at Ar atmosphere. The crystal structure is confirmed via X-ray diffraction (XRD) patterns at room temperature using a UltimaIV diffractometer with CuKα1 radiation (λ = 1.4506 Å) and a position-sensitive detector. The surface morphologies and corresponding energy-dispersive X-ray (EDX) of the SPEs are observed by scanning electron microscope (SEM, FEI NANOSEI 450).

Electrochemical Measurements

All electrochemical tests are conducted with standard coin cell (CR 2025). AC impedance spectroscopy is carried out by electrochemical workstation (CHI660E, Chenhua Instruments Co., China) at a frequency region of 0.1 Hz–100 MHz. Linear sweep voltammetry (LSV, 2.5 to 6.0 V with the scan rate of 10 mV^{-1}) and cyclic voltammetry (CV, − 0.5 to 6.0 V with the scan rate of 10 mV^{-1}) are conducted on the electrochemical workstation (CHI660E, Chenhua Instruments Co., China) with a stainless steel as working electrode and Li metal as a reference and counter electrode. The cycles are carried out by CT2001A cell test instrument (Wuhan LAND Electronic Co, Ltd). Coin cells sandwiching the SPEs between two stainless steel electrodes are assembled for lithium ion conductivity, which is calculated according to Eq. (1).

$$\sigma = \frac{d}{\mathrm{RA}} \tag{1}$$

where σ is conductivity, d is the thickness of SPEs, R is the resistance according to Nyquist plots, and A is the cross-section area. All solid-state lithium-ion batteries are assembled with $LiFePO_4$ cathode coupling with lithium metal anode. Typically, $LiFePO_4$, acetylene black, and polyvinylidene fluoride (7:2:1) are mixed with N-methyl-2-pyrrolidone (NMP). The mixture is coated on the aluminum foil and dried at 60 °C by vacuum overnight. The $LiFePO_4$ loading in the cathode is 2 mg cm^{-2}.

Results and Discussion

To illustrate the relation of lithium ion diffusivities in a Lewis base environment, the design concept is shown in Fig. 1a, in which a small amount of montmorillonite as Lewis base center is added into the PEO frames. Based on Lewis acid-base theory, the montmorillonite can perform as a contender with PEO chain to allow the lithium ion (Lewis acid) self-concentrated on the surface of montmorillonite due to the high absorbing energy [14]; thus, the lithium ions can escape the restraint of PEO chains. Furtherly, the low lithium-ion diffusion energy barrier (0.15 eV) on the surface of montmorillonite can enable the lithium-ion migration freely because the strategies for facilitating ion transport such as decreasing the lithium-ion diffusion energy barrier by introducing fast ion conductor are high necessary [30]. As presented in Fig. 1b, according to the results derived from its XRD curve, a hill-like peak can be observed, implying the crystallinity of PEO has been decreased to some degree, which confirmed the ability of montmorillonite to weaken lithium ion coordination with PEO chains. Carried the ionic conductivity farther is tested via AC impedance spectroscopy where coin cells are sandwiched the SPEs between two stainless steel electrodes. As shown in Fig. 1c, the results clearly demonstrate the advantage after montmorillonite incorporation that the ionic conductivity of SPEs could be greatly improved. Specially, the ionic conductivity (4.7 mS cm^{-1}) of SPEs with montmorillonite incorporation at 70 °C is

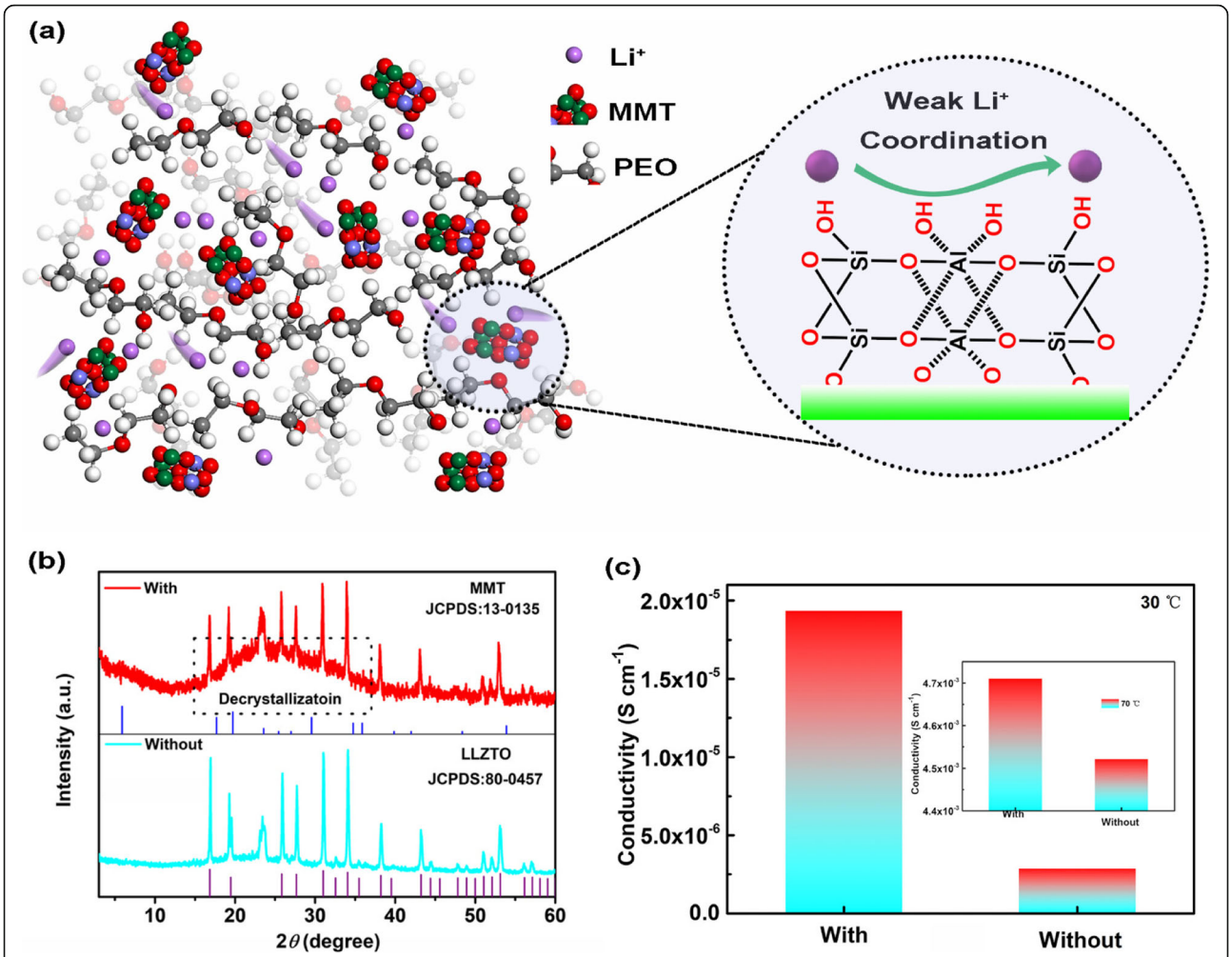

Fig. 1 Characterization of SPEs with montmorillonite doping: **a** The design concept that lithium ion can fast diffusion along the surface of montmorillonite. **b**, **c** The XRD and FTIR results of SPEs with or without montmorillonite particles, respectively

comparable with that of liquid electrolyte and would lead to the rapid transport of lithium ions.

Figure 2 presents the typical surface morphologies of the as-prepared SPEs. As shown in Fig. 2a, the SPEs without montmorillonite display uniform surfaces. The integrity of SPEs, however, was segmented into various irregular areas which may be caused by the solvent evaporation. Thereby, this structure increases the internal crystal interface of SPEs and slows down the transport of lithium ions. As contrast, this situation has been greatly optimized after montmorillonite involved in. The results show that the gaps between segmented SPEs have been filled due to the de-crystallization, presented in Fig. 1b. Furthermore, the feature element mapping of Si and Al confirmed the homogeneous distribution of montmorillonite particles embedded in the PEO matrix (Fig. 2c). Figure 2d shows the high-temperature performance of SPEs via thermogravimetric analysis. At low temperatures (< 150 °C), we observed a slight drop in weight, possibly from the evaporation of the residual solvent. Clearly, with or without montmorillonite, both of the SPEs present excellent thermal stability up to 370 °C.

Figure 3 presents the investigation of the electrochemical performances of SPEs. As shown in Fig. 3a, linear sweep voltammetry is employed to study the electrochemical window of SPEs before and after montmorillonite incorporation. Without montmorillonite, the oxidation process commences at 3.9 V. While the sweep can be extended to 4.6 V without an obvious current in the case after montmorillonite incorporation. The enhanced electrochemical stability can be attributed to the removed impurities such as water from the interface by the montmorillonite [31]. Correspondingly, the enhanced electrochemical stability is further confirmed via cyclic voltammetry (CV) scans that show the SPEs with montmorillonite deliver negligible redox current from 2.5 to 5 V (Fig. 3b). However, a contrasted phenomenon has been observed that the SPEs without montmorillonite increases the oxidation current,

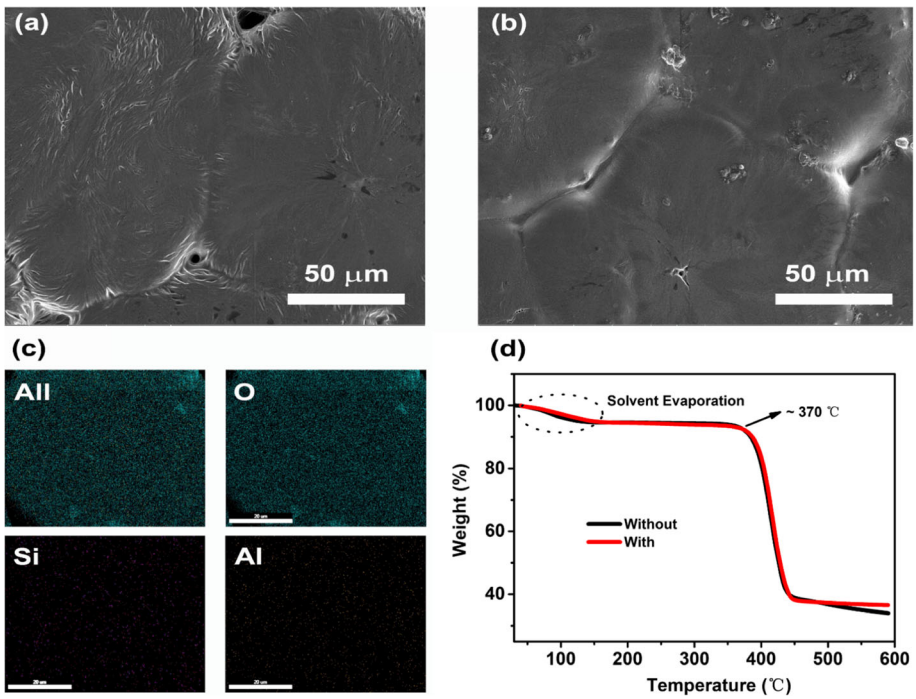

Fig. 2 SEM images of SPEs without (**a**) and with (**b**) montmorillonite doping. **c** The element mapping of SPEs with modification of montmorillonite. **d** TGA curve of SPEs from 30 to 600 °C at a rate of 10 °C min^{-1}

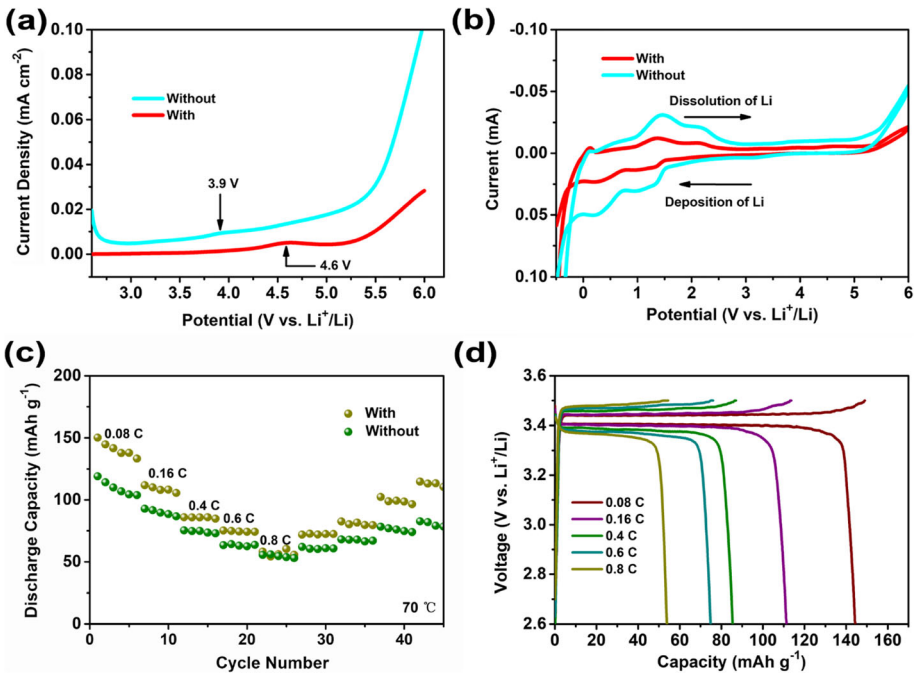

Fig. 3 The electrochemical performance of SPEs: LSV profiles (**a**), cycling performance (**b**), rate performance (**c**), and voltage profiles of SPEs after montmorillonite (**d**)

consisting with LSV results. Furtherly, the galvanostatic charging and discharging cycles of $LiFePO_4$ batteries are tested at 70 °C to confirm the actual applications of SPEs. As shown in Fig. 3c, the specific discharge capacity is 150.3 mAh g^{-1} with a high Coulombic efficiencies nearly 100% at 0.08 C, which is 88% of the theoretical value (170 mAh g^{-1}). Corresponding, the typical potential plateaus of LFP at 3.39 V and 3.44 V corresponding to discharge and charge can be clearly identified. As the current densities are increased to 0.16, 0.4, 0.6, and 0.8 C, the specific discharge capacities diminish to 111.8, 85.9, 75.2, and 58.2 mAh g^{-1}, respectively. Without montmorillonite, lower discharge capacity could be found as only 119.1 mAh g^{-1} at 0.08 C, which is 70% of the theoretical value. As the current density increases, the specific discharge capacities fast decrease to 92.8, 75.4, 63.4, and 55.5 mAh g^{-1} corresponding to 0.16, 0.4, 0.6, and 0.8 C, respectively. Therefore, all of the results clearly demonstrate again the benefits of montmorillonite to tailor all solid-state electrolyte with high ionic conductivity for actual application of lithium-ion batteries.

Conclusions

In summary, a small amount of montmorillonite as Lewis base center is added into the PEO frames to enable SPEs achieving high ionic conductive. The uniformly distribution of montmorillonite allows electrochemical window of SPEs improved from 3.9 to 4.6 V. This proposed strategy exhibits an excellent electrochemical performance that the prepared $LiFePO_4$ battery delivers a high discharge capacity of 150.3 mAh g^{-1} with the loading of 2 mg cm^{-2} at 70 °C, far exceeding the control sample (119.1 mAh g^{-1}) at a same current density of 0.08 C. All the results indicate the proposed strategy based on Lewis acid-base theory could be a promising method to achieve high-capacity and high-rate lithium-ion batteries.

Abbreviations

CV: Cyclic voltammetry; EDX: Energy-dispersive X-ray; LIBs: Lithium-ion batteries; LITFSI: Bis(trifluoromethanesulfonyl)imide; LLZTO: $Li_{6.4}La_3Zr_{1.4}Ta_{0.6}O_{12}$; LSV: Linear sweep voltammetry; MMT: Montmorillonite; NMP: N-methyl-2-pyrrolidone; PE: Polyethylene; PEO: Polyethylene oxide; PP: Polypropylene; SEM: Scanning electron microscope; SPEs: Solid polymer electrolytes; TG: Thermo-gravimetric; XRD: X-ray diffraction

Acknowledgements

Not applicable.

Authors' Contributions

YZ drafts the manuscript. YZ and YW make contribution on directing the experiments and data analysis. YZ and YW have taken part in the acquisition and interpretation of the data. YW formulates the idea of investigation and is the corresponding author of the work. Both authors read and approved the final manuscript.

Authors' Information

Not applicable.

Funding

None.

Availability of Data and Materials

All data are fully available without restriction.

Competing Interests

The authors declare that they have no competing interests.

Author details

[1]State Key Laboratory of Electronic Thin Films and Integrated Devices, University of Electronic Science and Technology of China, Chengdu 610054, China. [2]Chengdu No.7 High School, Chengdu 610041, China.

Received: 18 October 2019 Accepted: 12 November 2019
Published online: 05 December 2019

References

1. Liang Y, Zhao CZ, Yuan H, Chen Y, Zhang W, Huang JQ, Yu D, Liu Y, Titirici MM, Chueh YL, Yu H, Zhang Q (2019) A review of rechargeable batteries for portable electronic devices. InfoMat 1(1):6–32
2. Liu J, Bao Z, Cui Y, Dufek EJ, Goodenough JB, Khalifah P, Li Q, Liaw BY, Liu P, Manthiram A, Meng YS, Subramanian VR, Toney MF, Viswanathan VV, Whittingham MS, Xiao J, Xu W, Yang J, Yang XQ, Zhang JG (2019) Pathways for practical high-energy long-cycling lithium metal batteries. Nat Energy 4: 180–186
3. Liu L, Zhao H, Lei Y (2019) Advances on three-dimensional electrodes for micro-supercapacitors: a mini-review. InfoMat 1(1):74–84
4. Fan X, Liu X, Hu W, Zhong C, Lu J (2019) Advances in the development of power supplies for the internet of everything. InfoMat 1(2):130–139
5. Chen W, Lei T, Wu C, Deng M, Gong C, Hu K, Ma Y, Dai L, Lv W, He W, Liu X, Xiong J, Yan C (2018) Designing safe electrolyte systems for a high-stability lithium-sulfur battery. Adv Energy Mater 8(10):1702348
6. Chen D, Tan H, Rui X, Zhang Q, Feng Y, Geng H, Li C, Huang S, Yu Y (2019) Oxyvanite V3O5: a new intercalation-type anode for lithium-ion battery. InfoMat 1(2):251–259
7. Lv D, Zheng J, Li Q, Xi X, Seth F, Zimin N, Mehdi LB, Browning ND, Zhang JG, Graff GL, Liu J, Xiao J (2015) High energy density lithium–sulfur batteries: challenges of thick sulfur cathodes. Adv Energy Mater 5(16):1402290
8. Chen W, Qian T, Xiong J, Xu N, Liu X, Liu J, Zhou J, Shen X, Yang T, Chen Y, Yan C (2017) A new type of multifunctional polar binder: toward practical application of high energy lithium sulfur batteries. Adv Mater 29(12): 1605160
9. Chen W, Lei T, Qian T, Lv W, He W, Wu C, Liu X, Liu J, Chen B, Yan C, Xiong J (2018) A new hydrophilic binder enabling strongly anchoring polysulfides for high-performance sulfur electrodes in lithium-sulfur battery. Adv Energy Mater 8(12):1702889
10. Hu Y, Chen W, Lei T, Zhou B, Jiao Y, Yan Y, Du X, Huang J, Wu C, Wang X, Wang Y, Chen B, Xu J, Wang C, Xiong J (2019) Carbon quantum dots-modified interfacial interactions and ion conductivity for enhanced high current density performance in lithium-sulfur batteries. Adv Energy Mater 9(7):1802955
11. Lei T, Chen W, Huang J, Yan C, Sun H, Wang C, Zhang W, Li Y, Xiong J (2017) Multi-functional layered WS_2 nanosheets for enhancing the performance of lithium–sulfur batteries. Adv Energy Mater 7(4):1601843
12. Zhang W, Zhang S, Fan L, Gao L, Kong X, Li S, Li J, Hong X, Lu Y (2019) Tuning the LUMO energy of an organic interphase to stabilize lithium metal batteries. ACS Energy Lett 4(3):644–650
13. Lin Z, Xia Q, Wang W, Li W, Chou S (2019) Recent research progresses in ether- and ester-based electrolytes for sodium-ion batteries. InfoMat 1(3): 376–389
14. Lei T, Chen W, Hu Y, Lv W, Lv X, Yan Y, Huang J, Jiao Y, Chu J, Yan C, Wu C, Li Q, He W, Xiong J (2018) A nonflammable and thermotolerant separator suppresses polysulfide dissolution for safe and long-cycle lithium-sulfur batteries. Adv Energy Mater 8(32):1802441
15. Lei T, Chen W, Lv W, Huang J, Zhu J, Chu J, Yan C, Wu C, Yan Y, He W, Xiong J, Li Y, Yan C, Goodenough JB, Duan X (2018) Inhibiting polysulfide shuttling with a graphene composite separator for highly robust lithium-sulfur batteries. Joule 2(10):2091–2104

16. Miller TF, Wang ZG, Coates GW, Balsara NP (2017) Designing polymer electrolytes for safe and high capacity rechargeable lithium batteries. Acc Chem Res 50(3):590–593
17. Li Z, Huang HM, Zhu JK, Wu JF, Yang H, Wei L, Guo X (2019) Ionic conduction in composite polymer electrolytes: case of PEO:Ga-LLZO composites. ACS Appl Mater Interfaces 11(1):784–791
18. Yang C, Xie H, Ping W, Fu K, Liu B, Rao J, Dai J, Wang C, Pastel G, Hu L (2018) An electron/ion dual-conductive alloy framework for high-rate and high-capacity solid-state lithium-metal batteries. Adv Mater 31(3):1804815
19. Xu RC, Xia XH, Wang XL, Xia Y, Tu JP (2017) Tailored Li_2S–P_2S_5 glass-ceramic electrolyte by MoS_2 doping, possessing high ionic conductivity for all-solid-state lithium-sulfur batteries. J Mater Chem A 5(6):2829–2834
20. Kamaya N, Homma K, Yamakawa Y, Hirayama M, Kanno R, Yonemura M, Kamiyama T, Kato Y, Hama S, Kawamoto K, Mitsui A (2011) A lithium superionic conductor. Nat Mater 10(9):682–686
21. Kato Y, Hori S, Saito T, Suzuki K, Hirayama M, Mitsui A, Yonemura M, Iba H, Kanno R (2016) High-power all-solid-state batteries using sulfide superionic conductors. Nat Energy 1(4):16030
22. Kuhn A, Gerbig O, Zhu C, Falkenberg F, Maier J, Lotsch BV (2014) A new ultrafast superionic Li-conductor: ion dynamics in $Li_{11}Si_2PS_{12}$ and comparison with other tetragonal LGPS-type electrolytes. Phys Chem Chem Phys 16(28):14669–14674
23. Miara LJ, Ong SP, Mo Y, Richards WD, Park Y, Lee JM, Lee HS, Ceder G (2013) Effect of Rb and Ta doping on the ionic conductivity and stability of the garnet $Li^{7+}_{2x-y}(La_{3-x}Rb_x)(Zr_{2-y}Ta_y)O_{12}$($0 \leq x \leq 0.375$, $0 \leq y \leq 1$) superionic conductor: a first principles investigation. Chem Mater 25(15):3048–3055
24. Bron P, Johansson S, Zick K, Schmedt auf der Gunne J, Dehnen S, Roling B (2013) $Li_{10}SnP_2S_{12}$: an affordable lithium superionic conductor. J Am Chem Soc 135(42):15694–15697
25. Bachman JC, Muy S, Grimaud A, Chang HH, Pour N, Lux SF, Paschos O, Maglia F, Lupart S, Lamp P, Giordano L, Shao-Horn Y (2016) Inorganic solid-state electrolytes for lithium batteries: mechanisms and properties governing ion conduction. Chem Rev 116(1):140–162
26. Xiao R, Li H, Chen L (2015) High-throughput design and optimization of fast lithium ion conductors by the combination of bond-valence method and density functional theory. Sci Rep 5:14227
27. Xin S, You Y, Wang S, Gao HC, Yin YX, Guo YG (2017) Solid-state lithium metal batteries promoted by nanotechnology: progress and prospects. ACS Energy Lett 2(6):1385–1394
28. Savoie BM, Webb MA, Miller TF (1996) Enhancing cation diffusion and suppressing anion diffusion via Lewis-acidic polymer electrolytes. J Phys Chem Lett 8(3):641–646
29. Wieczorek W (1996) Composite polyether based solid electrolytes. The Lewis acid-base approach. Solid State Ionics 85(1–4):67–72
30. Chen W, Lei T, Lv W, Hu Y, Yan Y, Jiao Y, He W, Li Z, Yan C, Xiong J (2018) Atomic interlamellar ion path in high sulfur content lithium-montmorillonite host enables high-rate and stable lithium-sulfur battery. Adv Mater 30(40): 1804084
31. Zhang J, Zhao N, Zhang M, Li Y, Chu PK, Guo X, Di Z, Wang X, Li H (2016) Flexible and ion-conducting membrane electrolytes for solid-state lithium batteries: dispersion of garnet nanoparticles in insulating polyethylene oxide. Nano Energy 28:447–454

Publisher's Note